Attraction between pancake vortices and vortex molecule formation in the crossing lattices in thin films of layered superconductors

A. V. Samokhvalov,[1] A. S. Mel'nikov,[1] and A. I. Buzdin[2,3]

[1]*Institute for Physics of Microstructures, Russian Academy of Sciences, 603950 Nizhny Novgorod, GSP-105, Russia*

[2]*Condensed Matter Theory Group, LOMA, UMR 5798, Université Bordeaux 1, F-33405 Talence, France*

[3]*Institut Universitaire de France, Paris, France*

(Received 15 December 2011; revised manuscript received 9 February 2012; published 7 May 2012)

We study the intervortex interaction in thin films of layered superconductors for the magnetic field tilted with respect to the c axis. In such a case, the crossing lattice of Abrikosov vortices (AVs) and Josephson vortices appears. The interaction between pancake vortices, forming the AVs, with Josephson ones, produces the zigzag deformation of the AV line. This deformation induces a long-range attraction between Abrikosov vortices and, in thin films, it competes with another long-range interaction, i.e., with Pearl's repulsion. This interplay results in the formation of clusters of Abrikosov vortices, which can be considered as vortex molecules. The number of vortices in such clusters depends on field tilting angle and film thickness.

DOI: 10.1103/PhysRevB.85.184509 PACS number(s): 74.25.Ha, 74.78.−w

I. INTRODUCTION

The physics of vortices in layered superconductors is very rich and their study revealed many interesting phenomena.[1] Usually, the intervortex interaction is repulsive,[2] but in layered superconductors it occurs to be attractive at long distance in the plane defined by the vortex line direction and c axis (normal to the superconducting planes).[3–5] In the bulk sample, this attraction leads to the formation of the vortex pair. Then, a third vortex will be attracted by this pair, etc., and finally it results in the formation of a vortex chain. These vortex chains have been observed experimentally by the decoration technique in $YBa_2Cu_3O_7$,[6] scanning tunneling microscopy in $NbSe_2$,[7] and Lorentz microscopy measurements in $YBa_2Cu_3O_7$ (Ref. 8) (see Ref. 9 for a review).

However, the Lorentz microscopy experiments on a thin film of $YBa_2Cu_3O_7$ [with thickness D smaller than $(0.5 \div 1)$ μm] showed that the vortex chains disappear for slightly tilted magnetic field.[10] This is caused by the surface effect, which modifies the intervortex interaction, resulting in long-range intervortex repulsion as it has been demonstrated in the pioneering work[11] by Pearl in 1964. Indeed, in a thin film, we have an interplay between two different long-range potentials: (i) attraction of the tilted vortices ($U_{\rm att} \sim -1/R^2$) and (ii) the Pearl's repulsion ($U_{\rm rep} \sim 1/R$). By varying either the film thickness or the tilting angle, we can modify the balance between these interactions, which should determine energetically favorable vortex configurations in samples with thickness d comparable to the London penetration depth λ.[10] The Pearl's repulsion always dominates at large distances and, thus, the formation of an infinite vortex chain can become unfavorable. Adding vortices one by one, we can find an optimal number of vortices which can be arranged in a chain of a finite length. As a result, there appears an intriguing possibility to form a vortex structure consisting of finite-size chains, i.e., of vortex molecules.[10,12]

The scenario discussed above is applicable to the moderately anisotropic layered superconductors (such as $NbSe_2$, YBaCuO), when the magnetic field penetrates in the form of the tilted vortices. For strongly anisotropic superconductors such as $Bi_2Sr_2CaCu_20_{8+\delta}$ (BSCCO), the situation is qualitatively different and the tilted magnetic field penetrates in the form of the crossing lattice comprising the in-plane Josephson vortices (JVs) and perpendicular to the planes Abrikosov vortices (AVs). The AV in this case is a stack of the pancake vortices (PVs).[13] The interaction between PVs and JVs (Ref. 14) leads to the deformation of the perpendicular vortex line and results in the attraction between AVs and JVs. The most striking manifestation of these phenomena is the decoration of the JVs by the PVs visualized in BSCCO single crystals by the modern vortex imaging methods such as Lorentz microscopy,[8] high-resolution scanning Hall probe,[15] Bitter decoration techniques,[16] and magneto-optical measurements[17] (see also Ref. 9 as a review). Interestingly, the deformation of the AVs due to the intersection with JVs is responsible for a long-range attraction between vortex stacks,[18,19] which is quite similar to the AVs attraction in the case of moderately anisotropic superconductors.[3–5]

In this paper, we study how the Pearl's effect modifies the interaction between the deformed AVs in the film of a finite thickness. Special attention is paid to the conditions under which attraction between PVs in the crossing lattices exists and the dense vortex chains appear in tilted field. Keeping in mind BSCCO, we consider layered superconductors with a high anisotropy ratio $\gamma = \lambda_c/\lambda_{ab} \gg 1$, where λ_c is the penetration depth for currents along the c axis and λ_{ab} is the penetration depth for currents in the ab plane (parallel to the layers). To describe the interaction between pancakes, we choose to apply the approach of Josephson-decoupled superconducting layers,[13] which is known to be adequate in studies of the vortex lattice structure for very weak coupling of the layers $\lambda_J = \gamma s \gg \lambda_{ab}$, where the Josephson length $\lambda_J = \gamma s$ is the in-plane size of the Josephson core radius.[20] Namely, this case we will treat in this paper.

The paper is organized as follows. In Sec. II, we introduce a general formalism to describe vortices in strongly anisotropic layered superconductor and determine the shape of the zigzag vortex line. In Sec. III, we calculate the interaction between the zigzag lines in a thin superconducting film. In Sec. IV, we discuss the situation of low in-plane magnetic field and the conditions of vortex cluster formation.

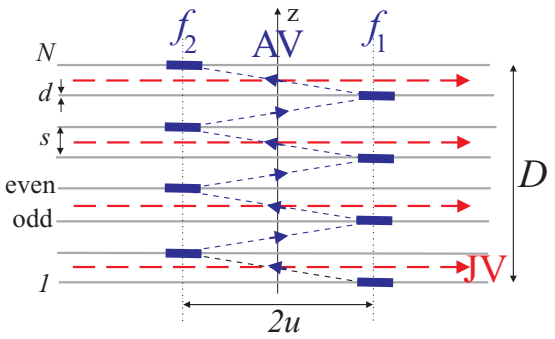

FIG. 1. (Color online) Zigzag deformation of the stack of pancakes due to interaction with the Josephson vortices (JV) in high parallel magnetic field ($B_x \gg H_0$), directed along the x axis. Here, d is a thickness of superconducting layer, s is a distance between the layers, n is the layer number, and u is the amplitude of deformation. Josephson vortices are shown by red dashed arrows.

II. ZIGZAG VORTEX LINE IN A FINITE STACK OF SC LAYERS

We start our study with the consideration of the equilibrium shape of PVs stack in the layered systems. The in-plane magnetic field $\mathbf{B}_\parallel = B_\parallel \mathbf{x}_0$ is assumed to penetrate inside the superconductor in the form of JVs, which interact with the PVs via the Josephson coupling.[14,21] Because of a very high anisotropy, the JV lattice is a triangular lattice strongly compressed along the c axis. In the high parallel magnetic field $B_\parallel > H_0 = \phi_0/\gamma s^2$, the dense triangular lattice of JVs produces zigzag displacement of PVs (Ref. 21) along the x axis, so that the pancake centers for each vortex line are positioned along the broken line (see Fig. 1).

A. Basic equations

Let us consider a finite stack of N superconducting (SC) layers. We denote the interlayer spacing as s and consider each of the N layers as a thin film with the thickness d much smaller than the London penetration depth λ. The field component perpendicular to the layers penetrates the SC film as a string of two-dimensional (2D) pancake vortices: each of these pancakes is centered at the point $\mathbf{r}_n = x_n\mathbf{x}_0 + y_n\mathbf{y}_0$ in the nth layer. Within the model of the stack of Josephson-decoupled SC layers, pancakes can interact with each other only via magnetic fields. The general equation for the vector potential $\mathbf{A}$ distribution in such a system reads as

$$\mathrm{rot}\,\mathrm{rot}\,\mathbf{A} = \frac{4\pi}{c}\sum_{n,m=1}^{N}\mathbf{J}_n^m(\mathbf{r})\,\delta(z-z_n), \tag{1}$$

where $\Lambda = \lambda^2/d = \lambda_{ab}^2/s$ is the effective penetration depth in a superconducting film, each nth SC layer coincides with the plane $z = z_n = ns$ $(1 \leqslant n \leqslant N)$. The sheet current at the nth layer created by the pancake at the mth layer takes the form

$$\mathbf{J}_n^m(\mathbf{r}) = \frac{c}{4\pi\Lambda}[\Phi(\mathbf{r}-\mathbf{r}_m)\,\delta_{nm} - \mathbf{A}^m(\mathbf{r},z_n)\,], \tag{2}$$

$\mathbf{A}^m(\mathbf{r},z)$ is the vector potential induced by the only pancake vortex located in the mth layer. The vector $\Phi(\mathbf{r})$ in Eq. (2) is given by the expression

$$\Phi(\mathbf{r}) = \frac{\phi_0}{2\pi}\frac{[\mathbf{z}_0\times\mathbf{r}]}{\mathbf{r}^2}, \tag{3}$$

and $\phi_0 = \pi\hbar c/e$ is the flux quantum. For the layered system without Josephson coupling, a general expression for the free energy can be written in the form

$$F = \frac{1}{8\pi}\int dV\left[(\mathrm{rot}\,\mathbf{A})^2 + \left(\frac{4\pi}{c}\right)^2\Lambda\sum_{n=1}^{N}\mathbf{J}_n^2(\mathbf{r})\,\delta(z-z_n)\right]. \tag{4}$$

The total vector potential $\mathbf{A}(\mathbf{r},z)$ and the sheet current in the nth layer $\mathbf{J}_n(\mathbf{r})$ produced by an arbitrary vortex line are the sum of the contributions induced by N pancakes

$$\mathbf{A}(\mathbf{r},z) = \sum_{m=1}^{N}\mathbf{A}^m(\mathbf{r},z), \quad \mathbf{J}_n(\mathbf{r}) = \sum_{m=1}^{N}\mathbf{J}_n^m(\mathbf{r}),$$

and can by found from Eqs. (1)–(3) using an approach similar to that proposed in Refs. 22 and 23 (see Ref. 12 for details).

B. Equilibrium shape of the zigzag vortex line

In order to find the equilibrium form of the vortex line in a finite stack of N superconducting layers under the influence of the crossing JVs lattice, we consider the relaxation of the set of the pancakes (one per layer) toward the equilibrium positions within the simplest version of the dynamic theory:

$$\eta\frac{d\mathbf{r}_n}{dt} = \sum_{m\neq n}\mathbf{F}_n^m + \mathbf{F}_n^J. \tag{5}$$

Here, η is the viscous drag coefficient, $\mathbf{F}_n^m$ is the interaction force acting on the pancake located in the nth layer by the sheet current $\mathbf{J}_n^m$ generated by the pancake positioned in the mth layer, and $\mathbf{F}_n^J$ is the resulting Lorentz forces acting on the nth pancake from the Josephson vortices.

The interaction forces $\mathbf{F}_n^m$ between two pancakes in layered superconductors was shown to be written as[12]

$$\mathbf{F}_n^m = \frac{\phi_0}{c}\left[\mathbf{J}_n^m\times\mathbf{z}_0\right] = \frac{\phi_0^2\,\mathbf{R}_{nm}}{8\pi^2\Lambda\lambda_{ab}R_{nm}} \times\left\{\frac{1}{R_{nm}}\delta_{nm} - \int_0^\infty dq\,J_1(qR_{nm})\,\frac{\alpha_n^m(q)\,g(q)}{Z(q)}\right\}, \tag{6}$$

where $J_1(\zeta)$ is the first-order Bessel function of the first kind, $\lambda_{ab}^2 = \Lambda s = \lambda^2 s/d$ is the penetration depth for the in-plane currents, $\mathbf{R}_{nm} = \mathbf{r}_n - \mathbf{r}_m$, and

$$Z(q) = 1 + 2q\Lambda/\tanh(qs).$$

The coefficients α_n^m obey the system of N linear equations

$$\begin{gathered} h(q)\,\alpha_1^m - \alpha_2^m = \delta_{1m}, \\ -\alpha_{n-1}^m + g(q)\,\alpha_n^m - \alpha_{n+1}^m = \delta_{nm},\ n\neq 1,N \\ -\alpha_{N-1}^m + h(q)\,\alpha_N^m = \delta_{Nm}, \end{gathered} \tag{7}$$

where we introduce two functions which depend on the wave number q:

$$\begin{aligned} g(q) &= 2\cosh(qs) + \sinh(qs)/\Lambda q, \\ h(q) &= \cosh(qs) + (1+1/\Lambda q)\sinh(qs). \end{aligned}$$

Without the JVs lattice, the magnetic coupling results in the absence of the in-plane displacement of pancakes $\mathbf{R}_{mk} = \mathbf{r}_m - \mathbf{r}_k = 0$ (i.e., the pancakes form a vertical stack). In the high-field limit $B_\parallel > H_0 = \phi_0/s\lambda_J$, all interlayer junctions are homogeneously filled with Josephson vortices, which form the dense triangular lattice. The period of the lattice in the z direction is equal to $2s$, which is much less than the period along the y axis $a = \phi_0/B_\parallel s \ll \lambda_J$. The sheet currents $\mathbf{J}_n = J_n(y)\mathbf{y}_0$ in the nth layer are given by the following continuity equations[20]:

$$\begin{aligned} dJ_1/dy &= j_0 \sin\theta_1, \quad dJ_N/dy = -j_0 \sin\theta_{N-1}, \\ dJ_n/dy &= j_0(\sin\theta_n - \sin\theta_{n-1}), \quad n \neq 1, N \end{aligned} \tag{8}$$

where $j_0 = c\phi_0/8\pi^2\gamma\lambda_{ab}^2\lambda_J$ is the Josephson interlayer critical current density, $\theta_n = \phi_{n+1} - \phi_n - (2\pi s/\phi_0)A_z$ is the gauge-invariant phase difference between the nth and $(n+1)$th layers, and $\phi_n(y)$ is the superconducting phase distribution at the nth layer. Considering the configuration of Josephson vortices shown in Fig. 1 in the high-field limit ($B_\parallel > H_0$) corresponding to strongly overlaping Josephson cores, we can put

$$\theta_n = 2\pi y/a + \pi(n-1). \tag{9}$$

These Josephson vortices result in the appearance of Lorentz forces $\mathbf{F}_n^J = F_n^J \mathbf{x}_0$ acting on the nth pancake:

$$\begin{aligned} F_1^J &= F_0/2, \quad F_N^J = -(-1)^N F_0/2, \\ F_n^J &= -(-1)^n F_0, \quad n \neq 1, N. \end{aligned} \tag{10}$$

The amplitude of the force

$$F_0 = \left(\frac{\phi_0}{4\pi\lambda_{ab}}\right)^2 \frac{2H_0}{\pi\gamma B_\parallel} \tag{11}$$

decreases with an increase of the in-plane magnetic field $B_\parallel$.

Considering the vortex line consisting of N pancakes, we start from the initial configuration of PVs arranged in the zigzag line $u_n = (-1)^{n+1}u$. The amplitude of the initial zigzag deformation

$$u \simeq \frac{\lambda_{ab}}{\beta \ln\beta}, \quad \beta = \frac{B_\parallel \lambda_J}{H_0 \lambda_{ab}} \gg 1 \tag{12}$$

is assumed to be small ($u \ll \lambda_{ab}$) and corresponds to the equilibrium form of the zigzag vortex in a bulk ($N \to \infty$) layered superconductor.[18,21] We measure all lengths in units of the penetration depth λ_{ab}, all forces in units of $\phi_0^2/8\pi^2\lambda_{ab}^2$, and normalize the time t by a relaxation time τ_0 proportional to the pancake viscosity η: $\tau_0 = 8\pi^2\lambda_{ab}^3\eta/\phi_0^2$. Typical values of the viscosity coefficient η for BSCCO can be found, e.g., in Ref. 24: $\eta/s \sim 10^{-8} \div 10^{-6}$ N s/m^2. These data suggest $\tau_0 \sim 10^{-13} \div 10^{-11}\, s$ for $s = 15$ Å and $\lambda_{ab} = 0.2\ \mu$m. As the system approaches its final force-balanced (equilibrium) configuration, the velocities of all pancake motions should vanish:

$$\lim_{t\to\infty} \frac{d\mathbf{r}_n}{dt} = 0, \qquad 1 \leqslant n \leqslant N.$$

Typically, the equilibrium configuration of pancakes is well established after a relaxation time of $t_r \sim 100 \div 200\,\tau_0$, which corresponds to the average velocity of a pancake $u/t_r \sim 10^2 \div 10^4\, sm/s$ for $B_\parallel \sim H_0$.

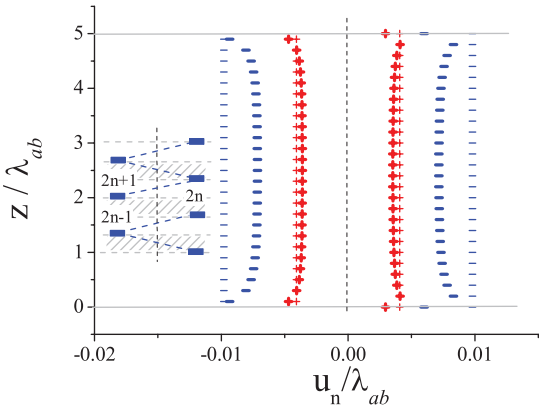

FIG. 2. (Color online) Equilibrium configurations of $N = 51$ pancakes in a finite stack in the presence of the Josephson vortices for two values of in-plane magnetic field $B_\parallel = H_0\,(-)$ and $B_\parallel = 2H_0\,(+)$. Small vertical stacks of symbols ($\pm$) show initial zigzag configuration of pancakes $u_n = (-1)^{n+1}u$ with the amplitude u defined by the relation (12). The inset shows schematically crossing PVs and JVs configuration. Patterned areas mark locations of the Josephson vortices. Here, $H_0 = \phi_0/\gamma s^2$, $\gamma = 300$, $s = 0.1\lambda_{ab}$, $\Lambda = 10\lambda_{ab}$.

In Fig. 2, we illustrate the equilibrium PVs configurations for two different values of the applied in-plane magnetic field $B_\parallel$. For small in-plane separation $u_n \ll \lambda_{ab} \ll \lambda_J$, the contribution of the stray-field potential to the overall pancake-pancake interaction can be neglected.[25] Since out-of-plane intervortex interaction extends over λ_{ab}/s layers, the attractive interaction $\sum \mathbf{F}_n^{m\neq n}$ between a single pancake vortex and a finite stack of pancakes is reduced near to the surface ($n \lesssim \lambda_{ab}/s$ and $N - n \lesssim \lambda_{ab}/s$) due to the missing planes for $z < 0$ and $z > D$, and the vortex line appears to have smaller line tension. The balance of forces $\mathbf{F}_n^J$ caused by the Josephson vortices and magnetic coupling between pancakes in different layers $\mathbf{F}_n^m$ results in a negligible deformation of homogeneous zigzag configuration of vortices in the layers at a distance $\sim \lambda_{ab}$ away from the top and bottom surfaces.

III. INTERACTION ENERGY OF TWO ZIGZAG VORTEX LINES

In this section, we derive general expressions for the interaction energy between two zigzag vortices in a thin film of layered superconductor taking into account both the long-range attraction and repulsion phenomena. The shape of the interacting vortex lines is assumed to be fixed and not affected by the vortex-vortex interaction potential. Certainly, such assumption is valid only in the limit of rather larger distances between the vortex lines when the effect of interaction on the vortex shape can be viewed as a small perturbation.

Using the gauge $\mathrm{div}\mathbf{A} = 0$ and the Fourier transform

$$\mathbf{A}(\mathbf{q},k) = \int d^2\mathbf{r}\, dz\, e^{i\mathbf{qr}+ikz}\mathbf{A}(\mathbf{r},z), \tag{13}$$

$$\mathbf{A}_n(\mathbf{q}) = \int d^2\mathbf{r}\, e^{i\mathbf{qr}}\mathbf{A}(\mathbf{r},z_n), \quad \mathbf{J}_n(\mathbf{q}) = \int d^2\mathbf{r}\, e^{i\mathbf{qr}}\mathbf{J}_n(\mathbf{r}), \tag{14}$$

one can rewrite the basic Eq. (1) for each vortex line in the momentum representation as follows:

$$(q^2+k^2)\,\mathbf{A}(\mathbf{q},k)=\frac{1}{\Lambda}\sum_n\,[\,\Phi_n(\mathbf{q})-\mathbf{A}_n(\mathbf{q})\,]\,e^{ikns}, \tag{15}$$

where $\Phi_n(\mathbf{q})=\Phi(\mathbf{q})\,e^{i\mathbf{q}\mathbf{r}_n}$. These equations can be reduced to the scalar form (see Ref. 12 for details)

$$f_n+\frac{1}{2q\Lambda}\sum_m \mathbf{e}^{-|n-m|qs}\,f_m=\mathbf{e}^{i\mathbf{q}\mathbf{r}_n}, \tag{16}$$

where we introduce the new functions $f_n(\mathbf{q})$:

$$\mathbf{J}_n(\mathbf{q})=\frac{c}{4\pi\Lambda}\,[\,\Phi_n(\mathbf{q})-\mathbf{A}_n(\mathbf{q})\,]=\frac{c}{4\pi\Lambda}\,\Phi(\mathbf{q})\,f_n(\mathbf{q}). \tag{17}$$

The solution of the linear system (16) for a fixed configuration of pancakes $\mathbf{r}_n$ determines the distribution of the vector potential $\mathbf{A}(\mathbf{r},z)$, which is created by an arbitrary vortex line in a finite stack of superconducting layers.

For two vortex lines, we can write the total vector potential and the total sheet current as superpositions of contributions coming from the first $(\mathbf{A}_n^{(1)},\mathbf{J}_n^{(1)})$ and second $(\mathbf{A}_n^{(2)},\mathbf{J}_n^{(2)})$ vortices. Calculating the interaction energy $\varepsilon_{\rm int}$ of vortex lines, we should keep in the free energy only the terms which contain the products of fields corresponding to different vortex lines. As a result, in the momentum representation, the general expression (4) for the free energy of the layered system without Josephson coupling reads as

$$\varepsilon_{\rm int}=\frac{1}{32\pi^3\Lambda}\sum_n\int d^2\mathbf{q}\big[\big(\Phi_n^{(1)}(\mathbf{q})-\mathbf{A}_n^{(1)}(\mathbf{q})\big)\times\Phi_n^{(2)}(-\mathbf{q})+\big(\Phi_n^{(2)}(\mathbf{q})-\mathbf{A}_n^{(2)}(\mathbf{q})\big)\Phi_n^{(1)}(-\mathbf{q})\big]. \tag{18}$$

For the particular case of two identical (parallel) vortex lines, which are shifted at the vector $\mathbf{R}=\mathbf{r}_n^{(2)}-\mathbf{r}_n^{(1)}$ $(n=1\div N)$ in the (xy) plane, we get following general expression for the interaction energy via the scalar functions $f_n(\mathbf{q})$ (Ref. 12):

$$\varepsilon_{\rm int}(\mathbf{R})=\frac{\phi_0^2}{16\pi^3\Lambda}\int\frac{d^2\mathbf{q}}{q^2}\,\cos(\mathbf{q}\mathbf{R})\sum_n f_n(\mathbf{q})\,e^{-i\mathbf{q}\mathbf{r}_n}. \tag{19}$$

The expression (19) and equations (16) determine the interaction energy of two identically bent vortex lines.

Further, we assume the centers of pancakes for each vortex line to be positioned at a zigzag line (see Fig. 1). For simplicity, we neglect a reduction of vortex line tension near the surface and assume that the amplitude of the zigzag deformation is the same for all layers $|u_n|=u\ll\lambda_{ab}$ and put

$$\mathbf{r}_n^{(1)}=(-1)^{n-1}u\mathbf{x}_0,\quad \mathbf{r}_n^{(2)}=\mathbf{r}_n^{(1)}+\mathbf{R}, \tag{20}$$

where the value u is determined by the expression (12). In the case of zigzag vortex line (20), Eq. (16) looks differently for odd and even layers:

$$f_n+\frac{1}{2q\Lambda}\sum_m^N \mathbf{e}^{-|n-m|qs}\,f_m=e^{i(-1)^{n+1}q_xu}. \tag{21}$$

It is convenient to introduce two new functions $f_{1k}(\mathbf{q})$ and $f_{2k}(\mathbf{q})$ for odd and even layers separately:

$$f_n=\begin{cases} f_{1k} & \text{if } n-\text{odd},\ k=(n+1)/2\\ f_{2k} & \text{if } n-\text{even},\ k=n/2\end{cases}$$

and rewrite Eq. (21) via the functions f_{1k} and f_{2k}:

$$f_{1,2k}+\frac{1}{2q\Lambda}\sum_m e^{-2|k-m|\,qs}\,f_{1,2m}+\frac{1}{2q\Lambda}\sum_m e^{-(2|k-m|+1)\,qs}\,f_{2,1m}=e^{\pm iq_xu}. \tag{22}$$

The interaction energy (19) expressed in terms of the scalar functions $f_{1k}(\mathbf{q})$ and $f_{2k}(\mathbf{q})$ reads as

$$\varepsilon_{\rm int}(\mathbf{R})=\frac{\phi_0^2}{16\pi^3\Lambda}\int\frac{d^2\mathbf{q}}{q^2}\,\cos(\mathbf{q}\mathbf{R})\times\sum_k^N[f_{1k}(\mathbf{q})\,e^{-iq_xu}+f_{2k}(\mathbf{q})\,e^{iq_xu}]. \tag{23}$$

The expression (23) and the system of algebraic equations (22) determine the interaction energy of two identical zigzag vortex lines which are shifted at the vector $\mathbf{R}$ in the (xy) plane.

A. Continuous limit

For the case of a large intervortex distance $R\gg s,u$, we may use the continuous limit for the solution of the problem (22) because for the relevant wave vectors $qs\ll1$ and $q_xu\ll1$. We introduce a continuous coordinate $z=2ks$ and continuous functions $f_{1,2}(\mathbf{q},z)$ defined at the interval $|z|\leqslant D/2$, where D is the total thickness of superconducting film. Thus, the linear system of equations (22) reduces to the following integral equations:

$$f_{1,2}(\mathbf{q},z)+\frac{1}{4q\Lambda s}\int_{-D/2}^{D/2}dz'\,e^{-q|z-z'|}\,f_{1,2}(\mathbf{q},z')+\frac{e^{-qs}}{4q\Lambda s}\int_{-D/2}^{D/2}dz'\,e^{-q|z-z'|}\,f_{2,1}(\mathbf{q},z')=e^{\pm iq_xu}. \tag{24}$$

In the continuous limit, the expression for interaction energy (23) takes form

$$\varepsilon_{\rm int}(\mathbf{R})=\frac{\phi_0^2}{32\pi^3\Lambda s}\int\frac{d^2\mathbf{q}}{q^2}\,\cos(\mathbf{q}\mathbf{R})\times\int_{-D/2}^{D/2}dz\,[f_1(\mathbf{q},z)\,e^{-iq_xu}+f_2(\mathbf{q},z)\,e^{iq_xu}]. \tag{25}$$

Equations (24) can be rewritten as differential ones

$$\frac{\partial^2 f_{1,2}}{\partial z^2}-\left(q^2+\frac{1}{2\Lambda s}\right)f_{1,2}-\frac{e^{-qs}}{2\Lambda s}\,f_{2,1}=-q^2\,e^{\pm iq_xu} \tag{26}$$

at the interval $|z|\leqslant D/2$ with the boundary conditions

$$\left(\frac{\partial f_{1,2}}{\partial z}+qf_{1,2}\right)_{D/2}=q\,e^{\pm iq_xu}, \tag{27}$$

$$\left(\frac{\partial f_{1,2}}{\partial z}-qf_{1,2}\right)_{-D/2}=-q\,e^{\pm iq_xu}. \tag{28}$$

Introducing the new functions

$$f_+(\mathbf{q},z)=\frac{f_1(\mathbf{q},z)+f_2(\mathbf{q},z)}{2q^2\cos(q_x u)},\quad f_-(\mathbf{q},z)=\frac{f_1(\mathbf{q},z)-f_2(\mathbf{q},z)}{2iq^2\sin(q_x u)},$$

we will get two identical decoupled equations for $f^{\pm}$ in the following form:

$$\frac{\partial^2 f_\pm}{\partial z^2}-p_\pm^2 f_\pm=-1, \tag{29}$$

where the wave numbers $p_\pm$ in the continuous limit ($qs\ll 1$) are

$$p_+^2\simeq q^2+1/\lambda_{ab}^2\,,\quad p_-^2\simeq q^2. \tag{30}$$

The boundary conditions (27) and (28) for the functions $f_\pm(\mathbf{q},z)$ at $z=\pm D/2$ read as

$$\left(\frac{\partial f_\pm}{\partial z}+qf_\pm\right)_{D/2}=1/q, \tag{31}$$

$$\left(\frac{\partial f_\pm}{\partial z}-qf_\pm\right)_{-D/2}=-1/q. \tag{32}$$

The solutions of Eqs. (29) satisfying the boundary conditions (31) and (32),

$$f_\pm(\mathbf{q},z)=\frac{1}{p_\pm^2}\left[1+\frac{(p_\pm^2-q^2)\cosh(p_\pm z)}{q\ (p_\pm\sinh L_\pm+q\cosh L_\pm)}\right], \tag{33}$$

result in the following expressions for the functions $f_{1,2}(\mathbf{q},z)$:

$$f_{1,2}(\mathbf{q},z)\simeq a(\mathbf{q},z)\cos(q_x u)\pm i\,\sin(q_x u), \tag{34}$$

where $L_\pm=p_\pm D/2$ and

$$a(\mathbf{q},z)=\frac{q^2}{p_+^2}\left[1+\frac{\cosh(p_+ z)}{q\lambda_{ab}^2\,(p_+\sinh L_+ + q\cosh L_+)}\right].$$

B. Interaction potential of two zigzag stacks

Using solutions (34), we may rewrite the expression for interaction energy (25) as follows:

$$\varepsilon_{\rm int}(\mathbf{R})=\frac{\phi_0^2}{16\pi^3\Lambda s}\int d^2\mathbf{q}\,\cos(\mathbf{qR})\left\{D\left[\frac{\cos^2(q_x u)}{p_+^2}+\frac{\sin^2(q_x u)}{q^2}\right]+\frac{2q\cos^2(q_x u)}{\lambda_{ab}^2 p_+^4(1+q/p_+\tanh L_+)}\right\}. \tag{35}$$

Performing in (35) the necessary integration, we finally obtain the following expression for the interaction energy of two identical zigzag pancake stacks, which are shifted at the vector $\mathbf{R}$ in the (xy) plane:

$$\varepsilon_{\rm int}(R)=\frac{\phi_0^2}{32\pi^2\Lambda s}\left\{D\left[2K_0\left(\frac{R}{\lambda_{ab}}\right)+K_0\left(\frac{R-2u}{\lambda_{ab}}\right)+K_0\left(\frac{R+2u}{\lambda_{ab}}\right)+\ln\left(\frac{R^2-4u^2}{R^2}\right)\right]+\frac{2}{\lambda_{ab}^2}\int_0^\infty\frac{dq}{\left(q^2+\lambda_{ab}^{-2}\right)^2}\frac{2J_0(qR)+J_0[q(R-2u)]+J_0[q(R+2u)]}{1+q/\sqrt{q^2+\lambda_{ab}^{-2}}\,\tanh^{-1}\left(D\sqrt{q^2+\lambda_{ab}^{-2}}/2\right)}\right\}, \tag{36}$$

where J_0 and K_0 are the Bessel and modified Bessel functions of zero order, respectively. The first term proportional to D in Eq. (36) describes the interaction between the zigzag stacks in the bulk layered system,[18] while the last term is responsible for the influence of film boundaries. In Fig. 3, we present some typical plots of the interaction energy per one layer $\varepsilon_{\rm int}/N$ versus the intervortex distance R for different thickness of the film D and the in-plane magnetic field B_x.

At long distances $R\gg\lambda_{ab}$, the modified Bessel functions decay exponentially, and a bulk short-range repulsion between two PVs stacks is negligibly small. The leading bulk contribution comes from the logarithmic term in (36), which describes an attraction between the zigzag PV lines. The last term in (36) describes long-range Pearl's repulsion, which decays as $1/R$ and results from the surface contribution to the energy. Assuming that the effect of the zigzag deformation $u\ll\lambda_{ab}$ is small, the long-range part of interaction energy (36) for $R\gg\lambda_{ab}$ can be written as

$$\varepsilon_{\rm int}(R)\simeq\frac{\phi_0^2}{8\pi^2}\left[-\frac{D\,u^2}{\lambda_{ab}^2\,R^2}+\frac{2}{R}+\frac{4u^2}{R^3}\right]. \tag{37}$$

One can observe an interplay between the long-range attractive and the repulsive forces between two zigzag deformed PV stacks, similar to the one between two tilted vortices in anisotropic SC films.[10,12] The last term in (37) describes a modification of long-range Pearl's repulsion due to zigzag deformation of the PVs stack. Certainly, in a bulk sample ($D\to\infty$), the Pearl's term in (37) vanishes, and at long distances the dominant interaction between the zigzag PV lines is an attraction.[18] As a result, in a bulk sample there always exists the minimum of the interaction potential, which realizes with logarithmic accuracy at $R_m\approx 2\lambda_{ab}\ln(\lambda_{ab}/u)$. However, the second term in (37) is very important even for rather thick films: for large R, the energy $\varepsilon_{\rm int}$ is always positive and corresponds to the vortex repulsion. With a decrease of the distance R, the attraction force comes into play and can result in the change of the sign of the energy at $R_0\approx Du^2/2\lambda_{ab}^2\gg\lambda_{ab}$, while short-range repulsion is still weak. Such behavior should be accompanied by the appearance of the minimum in the interaction potential. The condition $R_0>R_m$ gives us a rough estimate of the critical film thickness D_{cr} for which the minimum in the interaction potential can exist and the

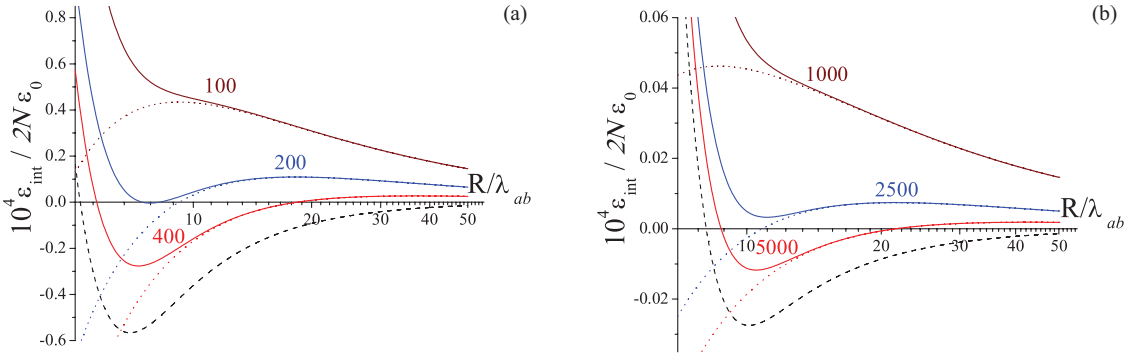

FIG. 3. (Color online) Typical plots of the interaction energy per layer $\varepsilon_{\rm int}(R)/2N\varepsilon_0$ [Eq. (36)] vs the distance R between two zigzag deformed stacks of pancakes for different values of in-plane magnetic field: (a) $B_\parallel/H_0 = 1$; (b) $B_\parallel/H_0 = 2$. The numbers near the curves denote the values of film thickness D/λ_{ab}. The dashed line shows the interaction energy between two zigzag vortices in bulk ($D \to \infty$) layered SC. Dotted lines show the long-range part of interaction energy (37). Here, $\varepsilon_0 = \phi_0^2/32\pi^2\lambda_{ab}$, $s = 0.01\,\lambda_{ab}$, $\gamma = 300$.

formation of vortex chains can be energetically favorable:

$$D_{cr} \approx 4\sigma\lambda_{ab}\beta^2(\ln\beta)^3 \sim \frac{4\sigma\lambda_J^2}{\lambda_{ab}}\left(\frac{B_\parallel}{H_0}\right)^2, \qquad (38)$$

where the constant σ is of the order unity. The more accurate criterion of attraction of zigzag PVs stacks should be based on the expression for the interaction energy (36) and may be found from the conditions

$$\varepsilon_{\rm int}(R) = \varepsilon'_{\rm int}(R) = 0.$$

The typical dependence of the critical film thickness D_{cr} as a function of in-plane magnetic field $B_\parallel$ is shown in Fig. 4. So, in the presence of a dense lattice of Josephson vortices, the AVs penetrate in the form of chains only for a large film thickness $D > D_{cr}$. Otherwise, if $D < D_{cr}$, the formation of the usual Abrikosov lattice of zigzag deformed stacks of PVs occurs. It is interesting to note that following (37), the intervortex attraction increases near the critical temperature of the superconducting transition T_c, when λ_{ab} becomes large (except for the region very close to T_c where the condition $\lambda_{ab} \ll \lambda_J$ is not satisfied). This behavior is in contrast with the moderately anisotropic case[12] when the critical thickness for intervortex attraction

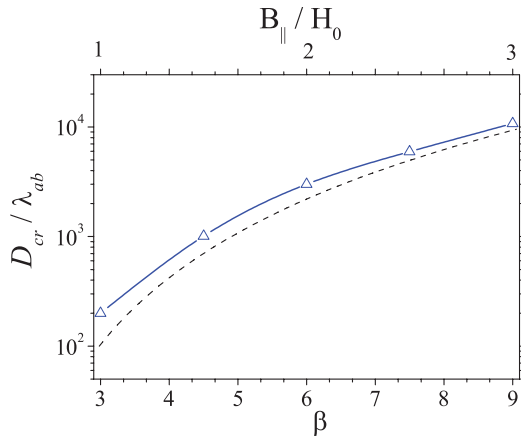

FIG. 4. (Color online) Critical film thickness D_{cr} as a function of in-plane magnetic field $B_\parallel$ ($\beta = B_\parallel\lambda_J/H_0\lambda_{ab}$). The dashed line shows the estimate of the critical film thickness (38). Here $s = 0.01\lambda_{ab}$, $\gamma = 300$, $\lambda_J = 3\lambda_{ab}$, $\sigma = 2$.

to be observed decreases near T_c and the repulsion between vortices prevails.

IV. DISCUSSIONS

In the high in-plane field limit $B_\parallel \gg H_0$ considered in Sec. III, the triangular lattice of JVs is so dense that the currents of adjacent JVs overlap strongly and the amplitude of the zigzag deformation decreases.[21] As a result, the critical thickness D_{cr} grows rapidly with an increase of the in-plane field $B_\parallel$ (see Fig. 4). Also, the potential dip in the intervortex interaction energy (36) strongly decreases with an increase of $B_\parallel$.[18] The optimal regime for the long-ranged attraction corresponds to $B_\parallel \sim H_0$. For typical values $s = 15$ Å, $\gamma = 300$, and $\lambda_{ab} = 0.2\,\mu$m, we obtain $H_0 \simeq 3$ T and $D_{cr} \sim 40\,\mu$m. Namely, this case of the intervortex interaction is presented in Fig. 3.

In the experiments,[26] the phase diagram of the vortex state in BSCCO single crystals was studied in strong oblique magnetic field ($B_\parallel \sim 0.6 \div 4.5$ T, $B_\perp \sim 5 \div 100$ Oe), and interesting anomalies related with the change of the vortex lattice structures have been observed. However, the direct observation of the interacting JVs and PVs by the Hall probe technique was performed in a weak in-plane magnetic field $B_\parallel \sim 20 \div 30$ Oe.[15] If the magnetic field $B_\parallel$ is small, the crossings between JVs and PVs are rare and the distance between Josephson vortices along the z axis becomes much larger than $2s$, as well as the distance between the deformed parts of the PVs line. Let us estimate the attraction between AVs in this limit. The Josephson vortices are well separated and positioned at the distance

$$\sqrt{\sqrt{3}\gamma\phi_0/2B_\parallel} \simeq s\sqrt{H_0/B_\parallel} \gg s$$

along the z axis. As has been demonstrated in Ref. 18, the contribution to the attraction from one crossing is

$$\tilde{\varepsilon}_{\rm att}(R) = -\frac{s\,\phi_0^2}{R^2}\left[\frac{\lambda_{ab}}{\lambda_J\ln(A\lambda_J/\lambda_{ab})}\right]^2, \qquad (39)$$

where $A \approx 3.5$ (see Ref. 14). Neglecting the effect of a zigzag deformation on the Pearl's repulsion, the long-ranged part of interaction energy $\tilde{\varepsilon}_{\rm int}(R)$ in the low-field limit $B_\parallel \ll H_0$ at

distances $R \gg \lambda_{ab}$ may be estimated as

$$\tilde{\varepsilon}_{\rm int}(R) \simeq \frac{\phi_0^2}{8\pi^2}\left[-\frac{D\,\tilde{u}^2}{\lambda_{ab}^2\,R^2}+\frac{2}{R}\right], \tag{40}$$

where the effective displacement[14,18]

$$\tilde{u} \simeq \frac{2\sqrt{2}\,\lambda_{ab}^2(B_\parallel/H_0)^{1/4}}{\lambda_J\,\ln(A\lambda_J/\lambda_{ab})} \tag{41}$$

grows slowly with increasing in-plane magnetic field $B_\parallel$. The expressions (40) and (41) result in the following estimate of the critical film thickness $\tilde{D}_{cr}$:

$$\tilde{D}_{cr} \sim \frac{\lambda_J^2\,\ln^2(A\lambda_J/\lambda_{ab})}{2\lambda_{ab}}\left(\frac{H_0}{B_\parallel}\right)^{1/2}. \tag{42}$$

As before, the case $B_\parallel \sim H_0$ is optimal for observation of intervortex attraction, and this case corresponds to the crossover between the regimes described by formulas (38) and (42). For typical experimental value of the in-plane magnetic field[15] $B_\parallel = 20 \div 30$ G, we obtain $\tilde{D}_{cr} \sim 70\ \mu$m.

Thus, the relations (38) and (42) give us the estimate of the threshold value of the thickness

$$D > \begin{cases} \tilde{D}_{cr} & \text{if } B_\parallel < H_0, \\ D_{cr} & \text{if } B_\parallel > H_0 \end{cases}$$

for which the minimum in the interaction potential can exist and the interplay between the long-range attraction and repulsion between zigzag vortex stacks lines in the films of layered superconductors takes place. We should note that the Pearl's interaction play an important role even for rather thick film; indeed, for the most favorable case $B_\parallel \sim H_0$, it completely masks the attraction for the film thicknesses smaller than $\sim(50 \div 200)\,\lambda_{ab}$.

The vortex attraction in bulk layered superconductors is known to result in the formation of infinite vortex chains. The long-ranged Pearl's repulsion of vortices in superconducting films always prevails at large distances and destroys the infinite chains.[10] The unusual intervortex interaction (36) leads to the unconventional vortex structures (vortex molecules or multiquanta flux lattice) discussed recently for moderately anisotropic superconductors in Ref. 12.

Qualitatively, all conclusions of references[10,12] are applicable for the case of crossing lattices we consider here. Similarly, the zigzags of PVs stacks can be arranged in vortex molecules. To estimate the size of such a molecule, let us find the cohesion energy of the equidistant chain of deformed PVs stacks. The perpendicular component of the magnetic field $B_\perp$ fixes the number M of AVs in the film, so that in the square film $W \times W$ it should be $M = B_\perp W^2/\phi_0$ vortices. We consider the case of small concentration of vortices when at large distances the intervortex interaction is given by Pearl's term. For roughly uniform vortex distribution (usual vortex lattice), the energy per one vortex can be estimated as $\varepsilon_0 \sim \phi_0 B_\perp W/4\pi^2$. If vortices form clusters with m vortices each, it may be demonstrated that interaction between clusters gives the same contribution ε_0 per one vortex. The remaining energy originates from the interaction between vortices inside the cluster, and for the case of a low in-plane magnetic field $B_\parallel \ll H_0$, it may be expressed via the long-ranged part of interaction energy $\tilde{\varepsilon}_{\rm int}$ (40):

$$\varepsilon_{\rm int}^m = \frac{1}{m}\sum_{i>j}^{m}\tilde{\varepsilon}_{\rm int}(R_{ij}), \tag{43}$$

where R_{ij} are the distances between ith and jth vortices in the chain molecule. Taking the characteristic distance between vortices in a cluster $\tilde{R}_m \approx 2\lambda_{ab}\ln(\lambda_J/\lambda_{ab})$, we find

$$\varepsilon_{\rm int}^m \sim \frac{\phi_0^2}{8\pi^2}\left[-\frac{D\,\tilde{u}^2}{\lambda_{ab}^2\tilde{R}_m^2}+\frac{2}{\tilde{R}_m}\ln m\right]. \tag{44}$$

Certainly, the cluster formation occurs if $\varepsilon_{\rm int}^m < 0$ and the number of vortices in the cluster is given by the expression

$$m \approx \exp\left(\frac{D\,\tilde{u}^2}{2\lambda_{ab}^2\tilde{R}_m}\right). \tag{45}$$

The condition $m > 1$ ($D\,\tilde{u}^2/2\lambda_{ab}^2\tilde{R}_m > 1$) gives us the low boundary of the in-plane magnetic field restricting the interval of vortex molecules existence

$$\frac{B_\parallel}{H_0} > \left[\frac{\lambda_J^2\,\ln^3(\lambda_J/\lambda_{ab})}{2D\,\lambda_{ab}}\right]^2. \tag{46}$$

For $D = 100\,\lambda_{ab}$, $\lambda_J = 3\,\lambda_{ab}$, and $H_0 = 3$ T, we obtain $B_\parallel > 60$ G. Note that the number of vortices m in the molecules rapidly increases as the in-plane magnetic field $B_\parallel$ grows.

Naturally, this scenario realizes only for low concentration of AVs when the average distance between vortices $\sqrt{\phi_0/B_\perp}$ is much larger than the intervortex distance in the chain $\tilde{R}_m$. In the opposite case, we may expect the existence of multiquanta flux lattice with several vortices per cell similar to the case of tilted vortices considered in Ref. 12.

We may conclude that the formation of the vortex molecules and the exotic vortex lattices with different number of vortices per unit cell should occur in the films with the thicknesses $D \gtrsim (10\text{–}100)\lambda_{ab}$, therefore, the most suitable technique to observe these structures seems to be the scanning tunneling microscopy, scanning Hall probe, or decoration.

ACKNOWLEDGMENTS

This work was supported, in part, by the Russian Foundation for Basic Research, by the Program "Quantum Physics of Condensed Matter" of RAS, by Russian Agency of Education under the Federal Program "Scientific and educational personnel of innovative Russia in 2009–2013," and by European IRSES program SIMTECH (Contract No. 246937). A.V.S. acknowledges the support of the program of LEA Physique Theorique et Matiere Condensee.

[1] G. Blatter, M. V. Feigel'man, V. B. Geshkenbein, A. I. Larkin, and V. M. Vinokuret, Rev. Mod. Phys. **66**, 1125 (1994).

[2] P. G. De Gennes, *Superconductivity of Metals And Alloys* (Benjamin, New York, 1966).

[3] A. I. Buzdin and A. Yu. Simonov, JETP Lett. **51**, 191 (1990) [Pis'ma Zh. Eksp. Teor. Fiz. **51**, 168 (1990)].

[4] A. M. Grishin, A. Yu. Martynovich, and S. V. Yampolskii, Sov. Phys.–JETP **70**, 1089 (1990) [Zh. Eksp. Teor. Fiz. **97**, 1930 (1990)].

[5]V. G. Kogan, N. Nakagawa, and S. L. Thiemann, Phys. Rev. B **42**, 2631 (1990).
[6]P. L. Gammel, D. J. Bishop, J. P. Rice, and D. M. Ginsberg, Phys. Rev. Lett. **68**, 3343 (1992).
[7]H. F. Hess, C. A. Murray, and J. V. Waszczak, Phys. Rev. Lett. **69**, 2138 (1992).
[8]A. Tonomura, H. Kasai, O. Kamimura, T. Matsuda, K. Harada, T. Yoshida, T. Akashi, J. Shimoyama, K. Kishio, T. Hanaguri, K. Kitazawa, T. Masui, S. Tajima, N. Koshizuka, P. L. Gammel, D. Bishop, M. Sasase, and S. Okayasu, Phys. Rev. Lett. **88**, 237001 (2002).
[9]S. J. Bending and M. J. W. Dodgson, J. Phys.: Condens. Matter **17**, R955 (2005).
[10]A. I. Buzdin, A. S. Mel'nikov, A. V. Samokhvalov, T. Akashi, T. Masui, T. Matsuda, S. Tajima, H. Tadatomo, and A. Tonomura, Phys. Rev. B **79**, 094510 (2009).
[11]J. Pearl, Appl. Phys. Lett. **5**, 65 (1964).
[12]A. V. Samokhvalov, D. A. Savinov, A. S. Mel'nikov, and A. I. Buzdin, Phys. Rev. B **82**, 104511 (2010).
[13]A. I. Buzdin and D. Feinberg, J. Phys. (Paris) **51**, 1971 (1990) [Zh. Eksp. Teor. Fiz. **76**, 1781 (1979)]; J. R. Clem, Phys. Rev. B **43**, 7837 (1991); K. Efetov, Sov. Phys.–JETP **49**, 905 (1979); S. N. Artemenko and A. N. Kruglov, Phys. Lett. A **143**, 485 (1990).
[14]A. E. Koshelev, Phys. Rev. Lett. **83**, 187 (1999).
[15]A. Grigorenko, S. Bending, T. Tamegai, S. Ooi, and M. Henini, Nature (London) **414**, 728 (2001).
[16]C. A. Bolle, P. L. Gammel, D. G. Grier, C. A. Murray, D. J. Bishop, D. B. Mitzi, and A. Kapitulnik, Phys. Rev. Lett. **66**, 112 (1991); I. V. Grigorieva, J. W. Steeds, G. Balakrishnan, and D. M. Paul, Phys. Rev. B **51**, 3765 (1995); M. Tokunaga, T. Tamegai, Y. Fasano, and F. de la Cruz, *ibid*. **67**, 134501 (2003).
[17]V. K. Vlasko-Vlasov, A. Koshelev, U. Welp, G. W. Crabtree, and K. Kadowaki, Phys. Rev. B **66**, 014523 (2002).
[18]A. Buzdin and I. Baladie, Phys. Rev. Lett. **88**, 147002 (2002).
[19]M. J. W. Dodgson, Phys. Rev. B **66**, 014509 (2002).
[20]L. Bulaevskii and J. R. Clem, Phys. Rev. B **44**, 10234 (1991).
[21]L. N. Bulaevskii, M. Maley, H. Safar, and D. Dominguez, Phys. Rev. B **53**, 6634 (1996).
[22]V. Pudikov, Phys. C (Amsterdam) **212**, 155 (1993).
[23]T. Pe, M. Benkraouda, and J. R. Clem, Phys. Rev. B **55**, 6636 (1997).
[24]A. E. Koshelev, Yu. I. Latyshev, and M. Konczykowski, Phys. Rev. B **74**, 104509 (2006).
[25]A. De Col, G. I. Menon, V. B. Geshkenbein, and G. Blatter, Phys. Rev. B **75**, 184532 (2007).
[26]J. Mirkovic, S. E. Savel'ev, E. Sugahara, and K. Kadowaki, Phys. Rev. Lett. **86**, 886 (2001); Phys. Rev. B **66**, 132505 (2002); M. Konczykowski, C. J. van der Beek, A. E. Koshelev, V. Mosser, M. Dodgson, and P. H. Kes, Phys. Rev. Lett. **97**, 237005 (2006).